

Reactive Organic Gas Emissions from Livestock Feed Contribute Significantly to Ozone Production in Central California

CODY J. HOWARD,[†] ANUJ KUMAR,^{†,‡} IRINA MALKINA,^{§,||} FRANK MITLOEHNER,[§] PETER G. GREEN,[†] ROBERT G. FLOCCHINI,[†] AND MICHAEL J. KLEEMAN^{*,†}

Department of Civil and Environmental Engineering, Crocker Nuclear Laboratory, and Department of Animal Science, University of California at Davis, 1 Shields Avenue, Davis California 95616

Received September 21, 2009. Revised manuscript received February 7, 2010. Accepted February 12, 2010.

The San Joaquin Valley (SJV) in California currently experiences some of the highest surface ozone (O_3) concentrations in the United States even though it has a population density that is an order of magnitude lower than many urban areas with similar ozone problems. Previously unrecognized agricultural emissions may explain why O_3 concentrations in the SJV have not responded to traditional emissions control programs. In the present study, the ozone formation potentials (OFP) of livestock feed emissions were measured on representative field samples using a transportable smog chamber. Seven feeds were considered: cereal silage (wheat grain and oat grain), alfalfa silage, corn silage, high moisture ground corn (HMG), almond shells, almond hulls, and total mixed ration (TMR = 55% corn silage, 16% corn grain, 8% almond hulls, 7% hay, 7% bran + seeds, and 5% protein + vitamins + minerals). The measured short-term OFP for each gram of reactive organic gas (ROG) emissions from all livestock feed was 0.17–0.41 g- O_3 per g-ROG. For reference, OFP of exhaust from light duty gasoline powered cars under the same conditions is 0.69 ± 0.15 g- O_3 per g-ROG. Model calculations were able to reproduce the ozone formation from animal feeds indicating that the measured ROG compounds account for the observed ozone formation (i.e., ozone closure was achieved). Ethanol and other alcohol species accounted for more than 50% of the ozone formation for most types of feed. Aldehydes were also significant contributors for cereal silage, high moisture ground corn, and total mixed ration. Ozone production calculations based on feed consumption rates, ROG emissions rates, and OFP predict that animal feed emissions dominate the ROG contributions to ozone formation in the SJV with total production of 25 ± 10 t O_3 day⁻¹. The next most significant ROG source of ozone production in the SJV is estimated to be light duty vehicles with total production of 14.3 ± 1.4 t O_3 day⁻¹. The majority of the animal

feed ozone formation is attributed to corn silage. Future work should be conducted to reduce the uncertainty of ROG emissions from animal feeds in the SJV and to include this significant source of ozone formation in regional airshed models.

1. Introduction

Ozone (O_3) is a persistent public health problem with serious economic consequences in the United States. In the years 2005–2007, more than 400 counties had 8 h average O_3 concentrations higher than 75 ppb (the most recent health-based National Ambient Air Quality Standard) (1). Three of six counties with the highest O_3 concentrations were located in California's San Joaquin Valley (SJV), while the remaining "top six" counties were located in Southern California (2). The severity of the O_3 problem in the SJV counties is puzzling given that they have a combined population of only 2.1 M compared to 14 M residents in the top Southern California counties. Higher temperatures, less summer cloud cover, and longer periods of stagnation in the SJV explain part of this trend, but even the most sophisticated computer models that account for all of these effects predict that O_3 concentrations in the SJV should be decreasing faster than currently observed in response to emissions control programs.

Ozone is produced by the photochemical reaction of oxides of nitrogen (NO_x) and reactive organic gases (ROGs). Lower ozone concentrations generally result from reductions in ROG emissions in urban areas. NO_x control is a more effective means to decrease ozone concentrations in regions where biogenic and other natural sources account for the majority of the ROG emissions. Photochemical model results based on current emissions inventories predict that NO_x control is a more efficient method for ozone reduction in the SJV, but that conclusion is subject to review as new ROG emissions sources are discovered. One possible cause for unexpected O_3 formation in the SJV is missing ROG emissions associated with the intensity of agricultural activities in the region. Almost 10% of the agricultural output for the entire United States comes from the SJV (3). The California Air Resources Board recently estimated that reactive organic gas (ROG) emissions from dairy cattle waste are the second largest source of O_3 formation in the SJV (with motor vehicle exhaust being the largest source) (4). Direct testing suggests that this initial estimate for dairy cattle waste is overstated since animal emissions do not contain ROGs with high ozone formation potential (OFP) (5, 6). Nevertheless, the OFPs of many other agricultural ROGs have not yet been tested, making agricultural emissions a high priority for further analysis.

Recent studies have identified animal feeds as one possible ROG source of agricultural OFP (7, 8). The ROG flux measured from silage and total mixed ration (TMR) was 2 orders of magnitude higher than comparable fluxes from animal waste (7). Chamber measurements confirm that animal feed ROG emissions are significantly higher than animal waste emissions and several of the animal feed ROG compounds have potentially high OFP (8). Neither of these previous studies directly quantified the OFP from animal feed or performed total ozone closure experiments, leaving the contribution of this source to regional ozone formation unknown.

The purpose of the present study is to directly measure the OFP of commonly used animal feeds and to estimate the importance of this ROG source for O_3 formation relative to other common ROG sources. A transportable smog chamber was used to measure OFP from seven feed types including one feed mixture under realistic agricultural conditions. Measured ROG emissions from feed placed into an envi-

* Corresponding author phone: (530) 752-8386; fax: (530) 752-7872; e-mail: mjkleeman@ucdavis.edu.

[†] Department of Civil and Environmental Engineering.

[‡] Crocker Nuclear Laboratory.

[§] Department of Animal Science.

^{||} Current address: California Air Resources Board, 1001 "I" Street, P.O. Box 2815, Sacramento, California 95812.

ronmental chamber were used to initialize model calculations of O₃ formation that were compared to measured values (ozone closure experiments). Finally, total emissions rates of ROG from animal feeding operations were estimated for the SJV so that the importance of this source could be judged relative to other common ROG sources that contribute to O₃ production.

2. Materials and Methods

2.1. Field Experiments. The OFP of sources too complicated to reproduce in the laboratory can be measured directly in the field using transportable smog chambers (5, 9). Ozone formation is measured by introducing a source gas into a well mixed chamber that contains background NO_x and reactive organic gases (ROG) that represents conditions in the region of interest. The background NO_x and ROG produce ozone when it is exposed to ultraviolet (UV) radiation. The OFP for the target source is defined to be the additional ozone that is formed when emissions from that source are added to the background mixture. The one drawback to transportable chambers is that they are usually smaller than laboratory chambers. The reduced size limits experiments to shorter times and the larger surface to volume ratios require extra care when accounting for wall effects. The benefits of making ozone measurements directly from complex sources far outweigh these limitations.

In the present study, a mobile ozone chamber assay (MOChA) was used to directly measure OFP from livestock feeds. The MOChA consists of a 1 m³ Teflon film reaction chamber housed within a wooden enclosure sitting on top of a modified trailer. The inner surface of the enclosure is covered with highly reflective aluminum sheeting, which helps to maximize UV irradiation of the reaction chamber. The UV irradiation is supplied by up to 26 UV lamps (model no. F40BL, Sylvania) with peak intensity at a wavelength of 350 nm. The lamps are mounted approximately 50 cm from the reaction chamber. The number of lamps was adjusted to produce $\sim 50 \pm 2$ W/m² of UV output, which is typical for conditions in Central California during the summer months. The intensity of UV irradiation was measured before and after each experiment using a photometer (model no. PMA-2111, Solar Light Co. Inc., Glenside, PA).

During a typical experiment, the reaction chamber was filled with source air using a Teflon diaphragm pump. The target concentration of background NO_x was added from a high pressure cylinder as a 95% NO₂/5% NO mixture by volume. The background ROG used in the present study consisted of a 55 \pm 1% ethene, 33 \pm 1% *n*-hexane, and 12 \pm 1% xylenes mixture by volume that was designed to simulate background ROG concentrations in the SJV during stagnation events. The composition of the background ROG was chosen to represent diluted urban plumes based on the "mini-surrogate" developed by Carter et al. (10). A grab canister sample (11) of the ROG concentrations was collected, the lights were turned on, and a three-hour ozone formation experiment was performed. Ozone, NO_x, relative humidity, and temperature measurements were made at regular intervals and logged to a computer. A second grab sample of ROG concentrations was collected at the end of the experiment, the lights were turned off, and the bag was evacuated and flushed using a clean air generator (model no. ZA-750-12, Perma Pure Inc., Toms River, NJ). Further details of the MOChA standard operating procedures and initial validation experiments are provided elsewhere (5).

Ozone formation experiments were performed on seven different types of feed obtained from a commercial local dairy. Those tested feeds included cereal silage (wheat grain and oat grain), alfalfa silage, corn silage, high moisture ground corn (HMGC), almond shells, almond hulls, and total mixed ration (TMR = 55% corn silage, 16% corn grain, 8% almond

hulls, 7% hay, 7% bran+seeds, and 5% protein + vitamins + minerals on a as-fed basis). Alfalfa silage was tested under two conditions: <1 week of fermentation and \sim 1 month of fermentation.

Feed samples were collected from trench silos on the dairy farm and moved to the testing facility in large double wrapped plastic bags. For cereal, alfalfa, and corn silage, a section of the silage face was removed so that the entire feed sample was collected from the anaerobic region. Air was removed from the plastic bags and they were sealed for transportation to the UC Davis Department of Animal Science where experiments were conducted. The test chamber was a 4.4 \times 2.8 \times 10.5 m sealed room with mechanically controlled ventilation. A detailed description of this facility can be found elsewhere (6). Feed samples were weighed and then placed in a circular bin that set on the floor of the chamber. The circular bin ensured that each feed type had the same exposed surface area (2.63 m²) during an experiment. The effective density of each of the feed types in kg per m³ was: corn silage (300 \pm 40), alfalfa silage (260 \pm 30), cereal silage (300 \pm 35), HMGC (640 \pm 70), almond shells (150 \pm 20), and almond hulls (160 \pm 20). After six minutes (the air residence time in the chamber), MOChA air samples were drawn from the ventilation outlet of the testing room through a 10 m Teflon tube. Canister samples, DNPH-silica cartridges (model no. 037500, Waters Corp, MA), and sorbent tube (model no. 226-119, SKC Inc., Eighty-Four, PA) samples were also collected inside the testing facility for supplemental ROG analysis. DNPH cartridges were eluted with acetonitrile and analyzed using high performance liquid chromatography (HPLC), while sorbent tube and canister samples were analyzed using gas-chromatography mass-spectrometry (GC-MS) (11-14). The ozone formation of each feed type was measured under two background ROG conditions: with background ROG added to the system and without background ROG. Initial NO_x concentrations were 50 \pm 5 ppb.

2.2. Model Calculations. Model calculations were used to perform ozone closure experiments and to estimate OFP under ROG/NO_x ratios other than those tested during experiments. Ozone closure experiments attempt to reconcile ozone measurements at the end of an experiment with ozone predictions made using only the ROG and NO_x concentrations measured at the beginning of an experiment. Extensive under-predictions of ozone formation would suggest the presence of unidentified ROG compounds with significant OFP (no such under-predictions were detected in the current study). Simulations were carried out using a modified version of the Caltech Atmospheric Chemistry Mechanism (CACM) (15). Modifications were made to CACM in order to accurately represent ethanol and acetaldehyde chemistry in rural conditions and to better simulate the spectrum of UV radiation emitted by the MOChA lamps (5). Model predictions for OFP were found to be in good agreement with previous OFP measurements for animal waste sources (5, 9). Likewise, in the present study model predictions are able to reproduce OFP for animal feed sources (see the Supporting Information (SI)).

3. Results and Discussion

A detailed list of the chemical species measured across all feed types and their lumped model category is provided in the SI. Alkanes (ALKL + ALKH), alkenes (OLEL + OLEH), and ketones (KETL + KETH) are lumped into two categories based on the number of carbon atoms in each molecule. Esters are lumped into one of the two ketone categories. Alcohols (ALCH) are represented with a single lumped category with the exception of explicit treatment for ethanol (ETOH). Acetaldehyde (ALD1) is also represented explicitly, while the rest of the aldehydes are grouped into two lumped categories representing higher molecular weight aldehydes (ALD2) and

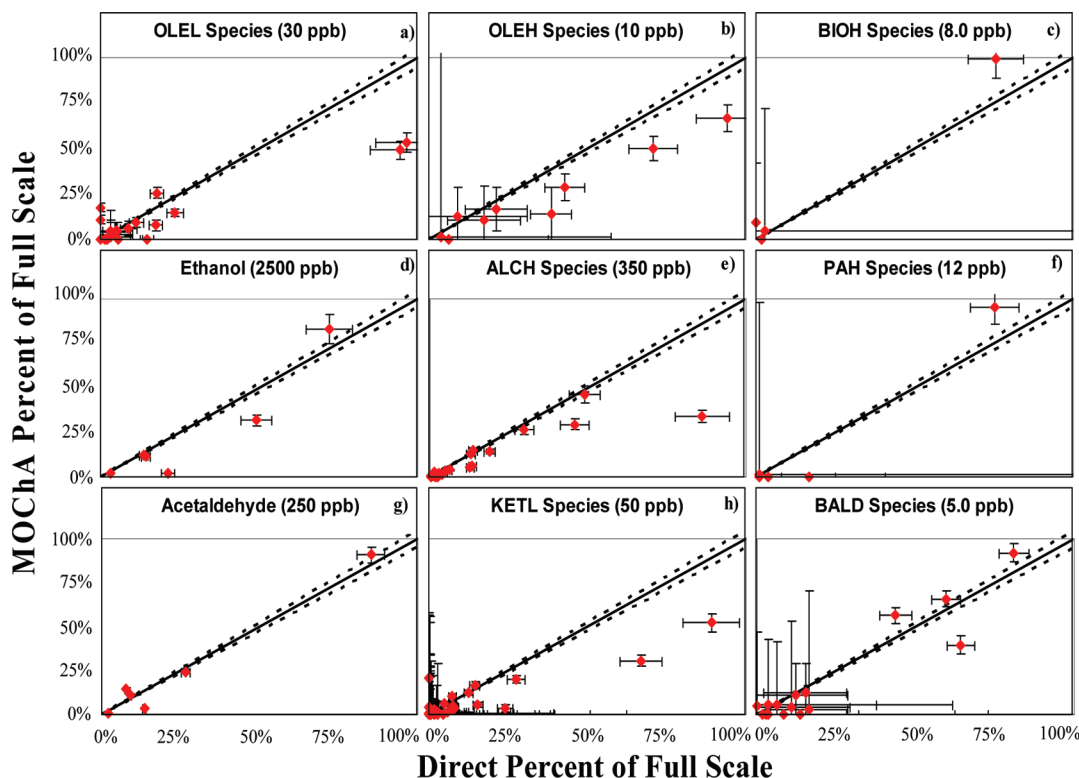


FIGURE 1. MOChA ROG canisters sample concentrations vs Direct ROG (from the test chamber) canister sample concentration for each lumped chemical species (concentrations in ppb). Note that each graph is from 0 to 100% of the maximum concentration, which is displayed in parentheses next to the species type.

cyclic aldehydes (BALD). Biogenics (BIOL + BIOH) and aromatic species (AROL + AROH) are lumped according to their SOA yield, whereas phenol (PHEN) is represented explicitly. A more detailed description of the CACM lumping scheme is provided elsewhere (5, 15), as are emissions rates for each of the chemical species (8).

Figure 1 depicts the differences between ROG species concentrations measured in the MOChA vs direct measurements in the feed testing facility. Each graph represents either an individual chemical species or a lumped chemical species category tracked by model calculations (see SI Table S1) with direct measurements of ROG on the x-axis and MOChA measurements of ROG on the y-axis. Regression analysis (see SI Table S2) was performed on MOChA vs direct measurements and the results show that those lumped species with average concentrations greater than 2 ppb had R^2 values above 0.84. The two species with the highest average concentration, ethanol (650 ppb) and acetaldehyde (60 ppb), had R^2 values of 0.91 and 0.98 respectively and the regression slope fell within one standard deviation of the 1:1 line (0.94 ± 0.27 and 1.04 ± 0.13 , respectively). Four of the eight lumped categories with average concentrations above 2 ppb (ALCH, OLEL, OLEH, and KETL) had regression slopes <0.68 with 95% confidence intervals below the 1:1 line consistent with losses to surfaces in the ventilation ducts and sampling lines. The two lumped species right at the 2 ppb threshold (BIOH and PAH) had regression slopes >1.21 but closer inspection shows that this result was driven by a single data point in each case. The corresponding 95% confidence intervals for the regression slopes are therefore very broad. Likewise, there was significant scatter for lumped species measured at concentrations <2 ppb, which resulted in lower correlation coefficients and broader confidence intervals for the regression slopes. The lower detectable concentration of the ROG measurement method was 1 ppb which explains the scattered behavior of measurements approaching this limit.

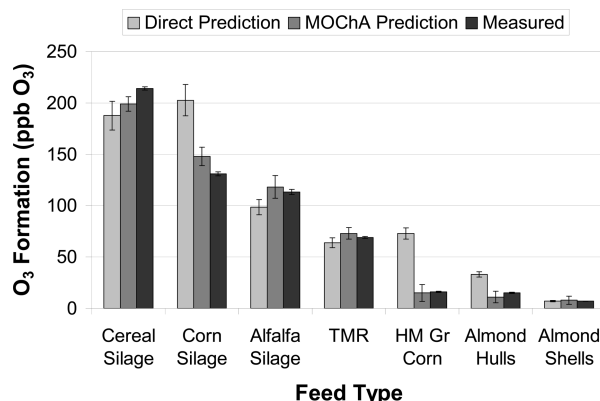


FIGURE 2. Ozone formation (ppb O_3) measured in each experiment vs model predictions using ROG samples from MOChA and Direct ROG samples from the feed testing facility.

Figure 2 illustrates the ozone formation (ppb- O_3) due to emissions from each animal feed vs the ozone formation predicted using CACM (ozone closure experiment). The figure depicts ozone formation under controlled conditions, where surface area of feed, ventilation rate in the chamber, and volume sampled remain constant across all feed types. By controlling these variables, the emissions from a feed type can be attributed to the actual flux from that feed. Simulations were conducted using the ROG profiles measured in the MOChA and the ROG profiles measured directly from the feed testing facility. For almost every feed type, the model predictions for ozone formation based on the MOChA ROG profiles are within uncertainty estimates to measured ozone formation in the MOChA. Ozone formation from corn silage, high moisture ground corn (HMGC), and almond hulls predicted using ROG profiles measured directly from the feed testing facility are higher than predictions based on

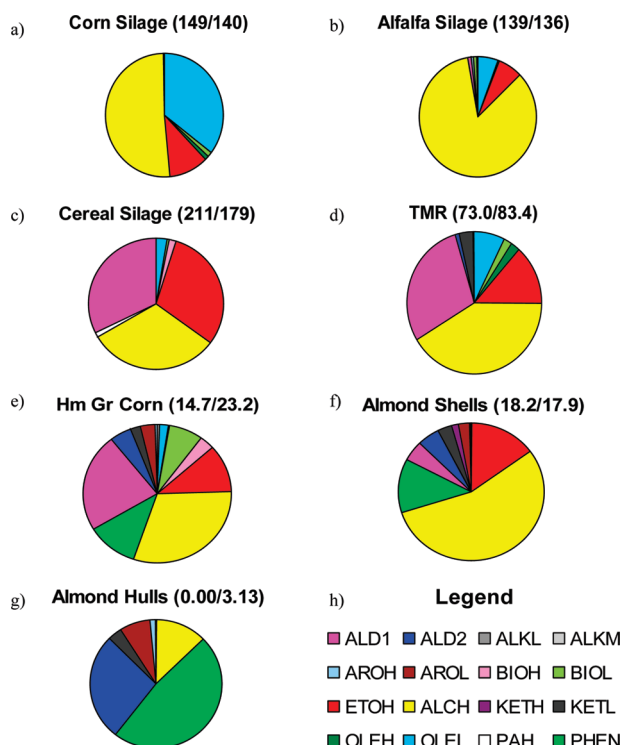


FIGURE 3. Contribution to total ozone formation from each lumped model species assuming additive behavior. Ozone formation associated with each species is calculated by removing that species from the ROG profile and observing the net reduction in ozone formation. The amount of ozone produced under the experimental conditions is listed after each subtitle (ppb O₃). The first value represents the measured total ozone formation, while the second value represents the predicted total O₃ formation using the sum from individual ROG subfractions. See the Supporting Information for an explanation of lumped model species codes.

MOChA ROG measurements. Concentrations of alcohol species were higher in the direct sample than the MOChA sample by a factor of 1.5, 5, and 10 for corn silage, almond hulls, and HMGC, respectively. Alcohol concentrations (ALCH + ETOH) account for roughly half of the ozone formation for these feed types. Multiplying the increased alcohol concentration by the expected ozone formation yields the difference in ozone formation between direct and MOChA samples for these three feed types (25% increase for corn silage, 300% for almond hulls, and 500% for HMGC). The influence of sampling line losses on these compounds must be considered when predicting the atmospheric ozone formation associated with these feeds.

Figure 3 illustrates the contribution that each lumped ROG category makes to ozone formation for each of the feeds. ROG contributions to ozone formation were calculated by removing the ROG from the feed profile and observing the reduction in predicted ozone production. This method assumes simple additive behavior (linear approximation) that does not completely describe the nonlinear photochemical system. The measured ozone formation and predicted ozone formation (sum of the individual ROG contributions) are displayed after the subtitle for each feed to convey the uncertainty introduced by the linear approximation. The relative error introduced by the linear approximation is <20% for feeds that produce >50 ppb O₃ under the experimental conditions (corn, alfalfa, cereal, TMR) with larger errors for feeds that produce <50 ppb of O₃ under the study conditions (HMGC, almond shells, almond hulls). Ethanol and especially larger alcohol species (ALCH) account for >50% of the ozone formation for most types of feed. Alkene species (OLEL) were

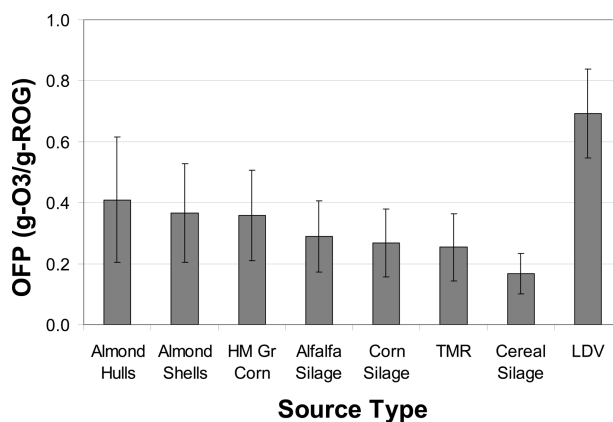


FIGURE 4. Calculated average O₃ formation potential (OFP) of the ROG emissions from animal feed sources and light duty gasoline-powered vehicles (LDV) expressed as g-O₃ produced per g-ROG emitted based on background NO_x and ROG concentrations. Uncertainty bars represent the range of conditions considered (see text).

significant contributors for corn silage and important in alfalfa silage and TMR. Acetaldehyde accounts for 25–30% of the ozone formation in cereal silage, TMR, and HMGC. Phenols account for significant ozone production for HMGC, almond shells, and almond hulls. Other important contributors to total ozone formation include the second lumped aldehyde category (ALD2), biogenic species, and aromatic species.

Model simulations were conducted to explore OFP of animal feeds under pollutant conditions expected in the SJV. Figure 4 displays the calculated ozone formation potential for feed in grams of ozone produced per gram of ROG emitted using the emissions measured in the current study. These values can be compared to the OFP of light duty gasoline-powered vehicle exhaust (LDV). The error bars in Figure 4 represent the range of conditions considered for each feed type, while the large bar represents the average between the estimates. The upper estimate represents urban concentrations in the SJV (NO_x = 75 ppb, ROG = 125 ppb), while the lower estimate represents rural conditions in the SJV (NO_x = 25 ppb, ROG = 62.5 ppb) (2). OFP is typically calculated using incremental reactivity, which compares the ozone formation of a reference mixture to the ozone formation of the reference mixture plus a small concentration of source ROG. Incremental reactivity can be defined for any point on an ozone isopleth, but at low NO_x and ROG conditions it is best to use the equal benefit incremental reactivity (EBIR), which is the point on the ozone isopleth where ROG and NO_x controls contribute equally to ozone reduction (16). Fortunately, the reference estimates for the SJV fall along this EBIR line for the NO_x conditions considered. The three silage feed types used in the experiments had OFP ranging from 0.17 to 0.29 g-O₃ per g-ROG. Total mixed ration, which contains both silage and other feeds, had the sixth highest OFP at 0.26 ± 0.11 g-O₃ per g-ROG. High moisture ground corn had the third highest OFP (0.36 ± 0.15 g-O₃ per g-ROG), almond shells had the second highest OFP (0.37 ± 0.16 g-O₃ per g-ROG), and almond hulls had the highest OFP (0.41 ± 0.21 g-O₃ per g-ROG). The OFP of LDV at EBIR conditions was calculated using CACM to be 0.69 ± 0.15 g-O₃ per g-ROG using published ROG emission estimates (17). These results demonstrate that under representative NO_x conditions, the OFP of feed sources are potentially important compared to LDV OFP.

Ozone formation potential quantifies the reactivity of each gram of ROG, but total emission estimates are needed to calculate total ozone formation within a region. Animal feed ROG emissions originate from storage silos and from feed placed in front of animals for their consumption. ROG

emission rates from the exposed face of storage silos and from feed placed in front of animals are calculated based on exposed feed surface area and measured flux rates (g ROG day⁻¹ m⁻²). SI Table S3 summarizes the flux emissions rates for different feeds inferred from test chamber measurements in the current study. Test chamber measurements were converted to flux rates using the following equation:

$$\text{flux} = \frac{CV}{\tau A} \quad (1)$$

where C is the measured concentration in the chamber, V is the chamber volume, τ is the time scale for air exchange in the room, and A is the surface area of exposed feed. Chamber measurements made at time $= \tau$ were still increasing to steady state values (achieved after time $= 3\tau$) and so the flux values are approximately 37% lower than the true initial emissions rates from the animal feeds. Continuous emissions flux measurements for corn silage made over a 24 h period indicate that steady state emissions decreases over time (18). A decrease of 37% from the initial emissions rate is achieved after approximately 4–5 h have passed. Hence, the emissions flux measurements are appropriate for an exposure time of 4–5 h. The corn silage emissions flux rates in the current study (1.66 ± 0.18 ROG g hr⁻¹ m⁻²) are in excellent agreement with direct flux rate measurements described by other investigators (1.8 ± 0.1 g ROG hr⁻¹ m⁻²) (7).

Total corn silage ROG emissions in the SJV were calculated assuming that almost all of the corn silage used in California is fed to dairy cattle and that most of the corn silage is kept in trench silos (not tower silos). The total daily feed consumption was estimated using statistics from the U.S. Department of Agriculture (19) (see SI Table S1).

ROG emissions from the exposed face of the trench silo (E_{face}) were calculated using the following equation:

$$E_{\text{face}} = \frac{M_{\text{feed}} A_{\text{face}} (\text{flux})}{\rho V_{\text{pile}}} \quad (2)$$

where M_{feed} is the total mass of silage feed consumed in the SJV each year ($1.0 \times 10^{10} \pm 5.0 \times 10^8$ kg) (19), ρ is the density of silage in the pile (300 ± 40 kg m⁻³) (20), V_{pile} is the volume of a representative silage pile ($1.0 \times 10^4 \pm 100$ m³) (20), A_{face} is the representative area of the silage pile face (90 ± 4.5 m²) (20), and flux is the ROG emissions flux appropriate for 4–5 h of exposure time (40 ± 2 g ROG day⁻¹ m⁻²) (measured this study).

Fugitive ROG emissions from corn silos (E_{spillage}) were calculated assuming that all of the ROG contained in the spoiled silage is released to the atmosphere using the following equation:

$$E_{\text{spillage}} = \frac{M_{\text{spoil}} \text{DM} f_{\text{EtOH_DM}}}{f_{\text{EtOH_ROG}}} \quad (3)$$

where M_{spoil} is the total amount of feed lost in the silo due to air spoilage (10% of total mass = $1.0 \times 10^9 \pm 5.0 \times 10^7$ kg yr⁻¹) (21), DM is the fraction of the silage that is dry matter (30%) (22), $f_{\text{EtOH_DM}}$ is the ratio of ethanol to dry matter in the feed (1.2%) (22), and $f_{\text{EtOH_ROG}}$ is the fraction of the ROG attributed to ethanol (EtOH) (55%) (8). This methodology predicts that fugitive ROG emissions can be calculated as 0.65% of the spoiled silage mass.

The ROG emission rate from feed placed in front of the animals (E_{manger}) was calculated assuming that the feed is available to the cows twenty-four hours a day using the equation:

$$E_{\text{manger}} = S_{\text{cow}} N_{\text{cow}} f_{\text{silage}} \text{flux} \quad (4)$$

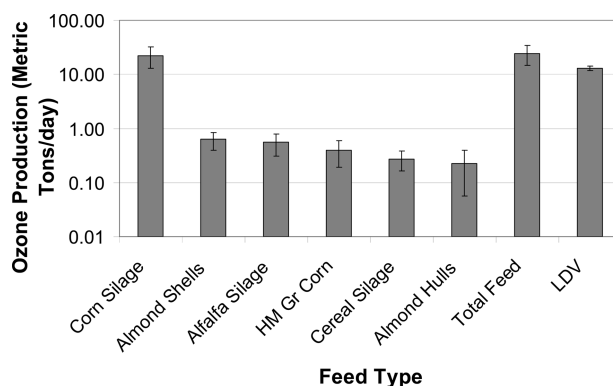


FIGURE 5. Total ozone production in metric tons per day for the various animal basic feed types vs light duty vehicles (LDV) in the SJV. Note that the y-axis is log scale. Calculations are based on OFP and total ROG emissions (see SI Table S1 for a summary of corn silage calculations).

where S_{cow} is the representative surface area of feed in front of each cow, N_{cow} is the number of cows in the SJV ($1.9 \times 10^6 \pm 1.9 \times 10^4$) (7), f_{silage} is the fraction of the feed composed of silage (50%) (see previous discussion of TMR composition), and flux is the ROG emissions flux appropriate for 4–5 h of exposure time (40 ± 2 g ROG day⁻¹ m⁻²) (measured this study). The E_{manger} was calculated using measurements from a typical dairy in the SJV (1200 cows, two barns each housing 600 cows, total length of feed line is 750 m, and effective cross-sectional width of feed line is 2.2 m). The result gives the average exposed feed surface area of 1650 m² for 1200 cows or 2.7×10^6 m² for 1.9 million cows in the SJV (23). Again, f_{silage} reduces the resulting surface area by half to account for approximately 50% corn silage used in TMR. All of the values needed to apply eqs 2–4 are summarized in SI Table S6 along with references for data sources.

The total ROG emissions from corn silage calculated using eqs 2–4 were 12.3 ± 1.9 t day⁻¹ (storage face) + 18.4 ± 1.8 t day⁻¹ (fugitive emission) + 53.1 ± 6.0 t day⁻¹ (feed in front of animals) yielding a total emissions rate of 83.8 ± 6.6 t day⁻¹. Multiplying ROG emissions by the OFP of corn silage (0.27 ± 0.11 g-O₃ per g-ROG) gives total ozone production in the SJV as 23 ± 9.5 t day⁻¹. Similar calculations of ozone production from the other feed sources were performed and the result is summarized in Figure 5. The estimated ozone formation from LDVs is also displayed in Figure 5 using published emissions estimates for this source (4). Traditional emissions inventory estimates have identified LDVs as the largest anthropogenic ROG source of ozone production in the SJV. The present calculations suggest that ozone production from animal feed ROG (25 ± 10 t day⁻¹) is nearly two times larger than ozone production from LDV ROG (14.3 ± 1.4 t day⁻¹) in this heavily polluted region. Corn silage accounts for 93% of the feed ozone production in the SJV. The next most significant category of feed is alfalfa silage contributing 2% to the SJV total.

All of the calculations described above are preliminary. Further refinements are needed to account for meteorological variables such as temperature, wind speed, and humidity. The relative importance of NO_x vs ROG control on ozone formation in the SJV must also be considered. The natural approach to evaluate these factors is the application of a regional air quality model that includes the newly recognized animal feed ROG emissions and then perturbs the system to consider the effectiveness of NO_x vs ROG emissions controls. The preliminary calculations shown in the present study clearly indicate that animal feed emissions are a significant source of ozone precursors in the SJV at current NO_x levels. Ozone control strategies in the SJV currently focus on NO_x control because previous calculations (without animal feed

ROG emissions) predicted this to be the most efficient strategy. If some measure of ROG control is deemed to be worthwhile when these new emissions are recognized, then future research should study how ROG emissions can be reduced from these essential animal feeds.

Acknowledgments

This research was funded by USDA Grant TM No. 2004-06138 with additional funding provided by the California Air Resources Board and the San Joaquin Valleywide Air Pollution Study Agency under contract 2000-05PM. The statements, opinions, findings, and conclusions of this paper are those of the authors and do not necessarily represent the views of the California Air Resources Board. The authors thank Chris Alaimo for his help with sample collection and analysis. Prof. Tom Young made available HPLC and GC-MS instruments. We are especially grateful to the cooperating dairy farm for providing animal feeds.

Supporting Information Available

Table S1 describes the assignment of individual ROG species to lumped CACM species, Table S2 summarizes regressions between MOChA vs Direct ROG measurements, Table S3 displays the emission flux rates for the various feed types in the test chamber, Table S4 lists the mass of feed used in chamber experiments, Table S5 lists the pH and total solids content of corn and alfalfa silage, Table S6 summarizes the data needed to calculate corn silage ROG emissions in the SJV, Figure S1 illustrates agreement between CACM predictions and MOChA measurements, Figure S2 illustrates calculated O₃ isopleths, Figure S3 illustrates the amount of each feed type used in California each year, Figure S4 displays measured concentrations of ROG species at or below the quantification threshold, and Figure S5 illustrates a picture of the MOChA apparatus. This material is available free of charge via the Internet at <http://pubs.acs.org>.

Literature Cited

- (1) *Proposed Revisions to Ozone National Standards*; U.S. Environmental Protection Agency: Washington, DC, 2007.
- (2) California Air Resources Board, pollutant summary. <http://www.arb.ca.gov/adam/cgi-bin/db2www/adamtop4b.d2w/start> (accessed March 2009).
- (3) *California Agricultural Statistical Review*; Department of Food and Agriculture: Sacramento, CA, 2009.
- (4) California Air Resources Board, Emissions Inventory Data. <http://www.arb.ca.gov/ei/emissiondata.htm> (accessed March 2009).
- (5) Howard, C. J.; Yang, W.; Green, P. G.; Mitloehner, F.; Malkina, I. L.; Flocchini, R. G.; Kleeman, M. J. Direct measurements of the ozone formation potential from dairy cattle emissions using a transportable smog chamber. *Atmos. Environ.* **2008**, *42* (21), 5267–5277.
- (6) Shaw, S. L.; Mitloehner, F. M.; Jackson, W.; Depeters, E. J.; Fadel, J. G.; Robinson, P. H.; Holzinger, R.; Goldstein, A. H. Volatile organic compound emissions from dairy cows and their waste as measured by proton-transfer-reaction mass spectrometry. *Environ. Sci. Technol.* **2007**, *41* (4), 1310–1316.
- (7) Alanis, P.; Sorenson, M.; Beene, M.; Krauter, C.; Shamp, B.; Hasson, A. S. Measurement of non-enteric emission fluxes of volatile fatty acids from a California dairy by solid phase micro-extraction with gas chromatography/mass spectrometry. *Atmos. Environ.* **2008**, *42* (26), 6417–6424.
- (8) Malkina, I. L.; Kumar, A.; Green, P. G.; Mitloehner, F. M. Identification and quantitation of volatile organic compounds emitted from dairy silages and other feedstuffs. *Atmos. Environ.* **2009**, submitted.
- (9) Howard, C. J.; Kumar, A.; Mitloehner, F.; Stackhouse, K.; Green, P. G.; Flocchini, R. G.; Kleeman, M. J. Direct measurements of the ozone formation potential from livestock and poultry emissions. *Environ. Sci. Technol.* **2010**, accepted for publication.
- (10) Carter, W. P. L.; Pierce, J. A.; Luo, D. M.; Malkina, I. L. Environmental chamber study of maximum incremental reactivities of volatile organic compounds. *Atmos. Environ.* **1995**, *29* (18), 2499–2511.
- (11) Kumar, A.; Viden, I. Volatile organic compounds: Sampling methods and their worldwide profile in ambient air. *Environ. Monit. Assess.* **2007**, *131* (1–3), 301–321.
- (12) Grosjean, E.; Green, P. G.; Grosjean, D. Liquid chromatography analysis of carbonyl (2,4-dinitrophenyl)hydrazones with detection by diode array ultraviolet spectroscopy and by atmospheric pressure negative chemical ionization mass spectrometry. *Anal. Chem.* **1999**, *71* (9), 1851–1861.
- (13) *Compendium Method TO-15, Determination of Volatile Organic Compounds (VOCs) in Air Collected in Specially-Prepared Canisters and Analyzed by Gas Chromatography/Mass Spectrometry (GC/MS)*; EPA/625/R-96/010b; U.S. Environmental Protection Agency, Office of Research and Development: Cincinnati, OH, 1999.
- (14) *Compendium Method TO-11A, Determination of Formaldehyde in Ambient Air Using Adsorbent Cartridge Followed by High Performance Chromatography (Active Sampling Methodology)*; EPA 625/R-96/010b; U.S. Environmental Protection Agency, Office of Research and Development: Cincinnati, OH, 1999.
- (15) Griffin, R. J.; Dabdub, D.; Seinfeld, J. H. Secondary organic aerosol - 1. Atmospheric chemical mechanism for production of molecular constituents. *J. Geophys. Res., [Atmos.]* **2002**, *107* (D17).
- (16) Carter, W. P. L. Development of ozone reactivity scales for volatile organic compounds. *J. Air Waste Manage. Assoc.* **1994**, *44* (7), 881–899.
- (17) Chang, C. C.; Lo, J. G.; Wang, J. L. Assessment of reducing ozone forming potential for vehicles using liquefied petroleum gas as an alternative fuel. *Atmos. Environ.* **2001**, *35* (35), 6201–6211.
- (18) Zhang, R.; Mitloehner, F.; El-Mashad, H.; Malkina, I.; Rumsey, T.; Arteaga, V.; Zhu, B.; Zhao, Y.; Goldstein, A.; Matross, D.; Hafner, S.; Montes, F.; Rotz, C. A. *Process-Based Farm Emission Model for Estimating Volatile Organic Compound Emissions from California Dairies*, Final Report to the California Air Resources Board for Project No. 05-344; California Air Resources Board: Sacramento, CA, 2009.
- (19) *Census of Agriculture, 2007*; U.S. Department of Agriculture: Washington, DC, 2007.
- (20) *Silage Pile Dimension Calculator*; University of Wisconsin Cooperative Extension: Madison, WI, 2009.
- (21) Holmes, B. J.; Muck, R. E. *Packing Bunkers and Piles to Maximize Forage*; University of Wisconsin Cooperative Extension: Madison, WI, 2007.
- (22) Sheperd, A. C.; Kung, L. Effects of an enzyme additive on composition of corn silage ensiled at various stages of maturity. *J. Dairy Sci.* **1996**, *79* (10), 1767–1773.
- (23) *Livestock Husbandry*; California Air Resources Board: Sacramento, CA, 2009.

ES902864U